A&A 570, A86 (2014)
DOI: 10.1051/0004-6361/201424275

Astronomy & Astrophysics

Pluto: improved astrometry from 19 years of observations⋆,⋆⋆,⋆⋆⋆

G. Benedetti-Rossi[1], R. Vieira Martins[1,⋆⋆⋆⋆], J. I. B. Camargo[1], M. Assafin[2,⋆⋆⋆⋆], and F. Braga-Ribas[1]

[1] Observatório Nacional/MCT, R. General José Cristino 77, CEP 20921-400 Rio de Janeiro - RJ, Brazil
e-mail: gustavorossi@on.br
[2] Observatório do Valongo/UFRJ, Ladeira Pedro Antonio 43, CEP 20.080-090 Rio de Janeiro - RJ, Brazil
e-mail: massaf@astro.ufrj.br

Received 26 May 2014 / Accepted 28 July 2014

ABSTRACT

Context. We present astrometric positions of Pluto, consistent with the International Celestial Reference System, from 4412 CCD frames observed over 120 nights with three telescopes at the Observatório do Pico dos Dias in Brazil, covering a time span from 1995 to 2013, and also 145 frames observed over 11 nights in 2007 and 2009 with the ESO/MPG 2.2m telescope equipped with the Wide Field Imager (WFI).
Aims. Our aim is to contribute to the study and improvement of the orbit of Pluto with new astrometric methods and positions.
Methods. All astrometric positions of Pluto were reduced with the Platform for Reduction of Astronomical Images Automatically (PRAIA), using the USNO CCD Astrograph Catalogue 4 (UCAC4) as the reference catalog. We also used the planetary ephemeris DE421+plu021 for comparisons. The positions were corrected for differential chromatic refraction. The (x, y) center of Pluto was determined from corrections to the measured photocenter, which was contaminated by Charon. The corrections were obtained with an original procedure based on analytical expressions derived from a two-dimensional Gaussian function i.e. the point spread function PSF fitted to the images to derive the (x, y) measurements.
Results. We obtained mean values of 4 mas and 37 mas for right ascension and declination, and standard deviations of σ_α = 45 mas and σ_δ = 49 mas, for the offsets in the sense observed minus ephemeris position, after the corrections. We confirm the presence of a linear drift in the ephemeris declinations from 2005 on, also obtained from stellar occultations.
Conclusions. We present astrometric positions of Pluto for 19 years of observations in Brazil. The positions, corrected for differential chromatic refraction and Pluto/Charon photocenter effects, presented the same behavior as obtained from stellar occultations, with a drift in declinations of about 100 mas since 2005. The results indicate that the DE421 Pluto ephemeris used in this work need to be corrected.

Key words. planets and satellites: individual: Pluto – atmospheric effects – methods: data analysis – methods: analytical – methods: numerical – astrometry

1. Introduction

Since its discovery in 1930 (Leonard 1930; Slipher 1930; Tombaugh 1946), Pluto remains one of the most interesting objects of study in the solar system. Physical and dynamical parameters have changed a lot during the years. Its mass, for example, was first calculated by Nicholson as 0.94 Earth masses (Nicholson & Mayall 1931), and changed to 0.0017 Earth masses after the discovery of Charon in 1978 (Christy & Harrington 1978; Harrington & Christy 1980; Walker 1980). Today, Pluto is the main representative body of the trans-Neptunian objects (TNOs), the only one with a known atmosphere (Elliot et al. 1989; Stern 1992) and with a system of 5 known satellites: Charon, Hydra, Nix (Weaver et al. 2006), Kerberos (Showalter et al. 2011) and Styx (Showalter et al. 2012).

Until the arrival of the NASA New Horizons spacecraft in 2015, almost all information on Pluto comes from ground-based observations. In particular, astrometric observations from the ground are affected by our atmosphere and the derived positions may present, for example, offsets caused by the difference in color of the light that comes from Pluto and from the background stars (chromatic refraction). Since it depends on the hour angle, meridian circle observations – like the ones from the United States National Observatory (USNO), for example – do not need such correction for right ascension. However, there is still a small correction in declination to be applied. The determination of the position of Pluto may also be affected by Charon's light, since its angular separation from Pluto is less than 1″. If there is not enough angular resolution, what we see is the mixed photocenter of the Pluto/Charon system, not the photocenter of Pluto itself, and not the barycenter (center of mass) of Pluto/Charon, for that matter. Each of these two effects may induce, as shown in this work, an offset of up to 100 mas on Pluto's position.

Comparing the planetary and lunar ephemerides DE421 (Folkner et al. 2009) – the most modern JPL DE at the time this work started – to stellar data occultation from Assafin et al. (2010), it is possible to see that there has been a drift in Pluto's declination of about 100 mas since 2005. Stellar occultations are the most efficient method, from the ground, to provide the

⋆ Full Table 4 is only available in electronic form at the CDS via anonymous ftp to cdsarc.u-strasbg.fr (130.79.128.5) or via http://cdsarc.u-strasbg.fr/viz-bin/qcat?J/A+A/570/A86
⋆⋆ Based on observations made at Laboratório Nacional de Astrofísica (LNA), Itajubá-MG, Brazil.
⋆⋆⋆ Partially based on observations through the ESO runs 079.A-9202(A), 075.C-0154, 077.C-0283, and 079.C-0345.
⋆⋆⋆⋆ Associate researcher at Observatoire de Paris/IMCCE, 77 Avenue Denfert Rochereau, 75014 Paris, France.

temperature and density profiles of Pluto's atmosphere and to determine the dimension of Charon and its relative distance to Pluto with kilometric accuracy (Sicardy et al. 2012). Accounting for the declination drift was essential to predicting new stellar occultations since 2005 and to the development of new ephemerides, with special concern regarding the New Horizons space mission.

Motivated by this context, we reduced and analyzed our data set of astrometric observations of almost 19 years, obtained at the Observatório do Pico dos Dias (OPD, IAU code 874), Brazil. We also used observations made at the ESO/MPG with the 2.2 m telescope equipped with the Wide Field Imager (WFI). We applied two astrometric post reduction corrections to the positions, considering first the differential chromatic refraction and after the mixed Pluto/Charon photocenter. Both corrections are described in the next sections. In particular, we used an original approach to correct Pluto's center based on a rigorous treatment of the point spread function (PSF) of the mixed Pluto/Charon images. We also derived 16 precise independent UCAC4-based positions for Pluto, based on specific OPD observations of occulted stars and on stellar occultation data. Our results confirm previous indications from stellar occultations given by Assafin et al. (2010) and put ephemerides errors in greater evidence. Our new precise positions allows for new adjustments of Pluto's orbit, which can be used, for instance, for the navigation of the New Horizons spacecraft.

New adjustments in Pluto's orbit were then implemented on recent (at the time of this writing) ephemerides: NASA/JPL – DE430 (Folkner et al. 2014), Observatoire de Paris/IMCCE – INPOP13c[1], and ODIN1 (Beauvalet et al. 2013), where a better agreement was obtained with respect to the positions of Pluto presented here. It should be noted, however, that INPOP13c and ODIN1 made use of the stellar occultation data and DE430 made use of both stellar occultation data and the positions presented here.

In Sect. 2 we describe the observations. The astrometric reductions and details of the post corrections are presented in Sect. 3. The final positions are given in Sect. 4. Comparisons with ephemerides and with results from stellar occultations are made in Sect. 5. Conclusions are drawn in Sect. 6. The analytical/numerical basis of the Pluto/Charon photocenter correction is described in Appendix A.

2. Observations

2.1. OPD

Our observations consist on 4412 CCD frames distributed over 120 nights covering a time span from 1995 and 2013. They were obtained at the Observatório do Pico dos Dias, Brazil (OPD, IAU code 874)[2], at geographical longitude +45° 34′ 57″ (W), latitude −22° 32′ 04″ (S) and an altitude of 1864 m. Near the city of Itajubá in the state of Minas Gerais, this site is under the auspices of a national astrophysics laboratory, the Laboratório Nacional de Astrofísica (LNA). Two telescopes of 0.6 m diameter (Zeiss and Boller & Chivens) and one of 1.6 m diameter (Perkin-Elmer) were used in the program. Typical seeing for our OPD observations is around 1.4″, as shown by Fig. 1.

Most of the observations were made without the use of filters (56 nights), but V (15 nights), R (29 nights), and I (23 nights) band pass filters (Bessell 1990) were also used.

[1] See http://www.imcce.fr/inpop/download13c.php and http://www.imcce.fr/inpop/inpop13c.pdffordetails.

[2] Website: http://www.lna.br/opd/opd.html – in Portuguese

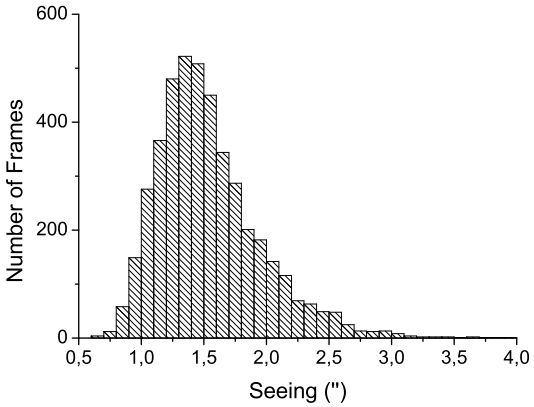

Fig. 1. Distribution of the seeing from our OPD observations.

Table 1. Exposure time for each telescope used on our observations.

Telescope	Exposure times typical[a] (s)	range[b] (s)
Perkin-Elmer (1.6 m)	30	10–120
Zeiss (60 cm)	60	15–80
Boller & Chivens (60 cm)	60	15–120
ESO/MPG/WFI (2.2 m)	30	30

Notes. [(a)] Typical values without filter for the telescopes at OPD and with R filter for the 2.2 m ESO telescope. [(b)] Exposition time range considering all filters used on the observations.

2.2. ESO La Silla

We also acquired 145 frames at the 2.2 m telescope at ESO/MPG (IAU code 809) with the WFI and standard broadband R filter (filter number 844, $\lambda_{\rm central}$ = 651.725 nm, $FWHM$ = 162.184 nm) during three runs: September 2007, October 2007, and May 2009. Typical exposure times for each telescope are presented in Table 1. The distribution of our observation nights is presented in Fig. 2.

In the time span of the observations, the right ascension of Pluto changed from about $15^{\rm h}\,50^{\rm m}$ to $18^{\rm h}\,50^{\rm m}$, and its declination from about −06° 30′ to −20° 00′, so Pluto was very suitable for observations from the OPD and ESO sites.

3. Astrometry

3.1. Primary (α, δ) reductions

Prior to the astrometric reductions, the frames were photometrically calibrated with auxiliary bias and flat-field frames by means of standard procedures using IRAF[3].

The astrometric reductions were made by the use of the Platform for Reduction of Astronomical Images Automatically (PRAIA; Assafin et al. 2011). The (x, y) measurements were performed with two-dimensional circular symmetric Gaussian fits within 1 full width half maximum (FWHM = seeing). Within 1 FWHM, the image profile is reliably described by a Gaussian profile and is free from wing distortions, which jeopardize the center determination. PRAIA automatically recognizes catalog stars and determines (α, δ) with a number of models relating the (x, y) measured and (X, Y) standard coordinates projected in the sky tangent plane. We used the UCAC4 (Zacharias et al. 2013) as the practical representative of the International

[3] Website: http://iraf.noao.edu/

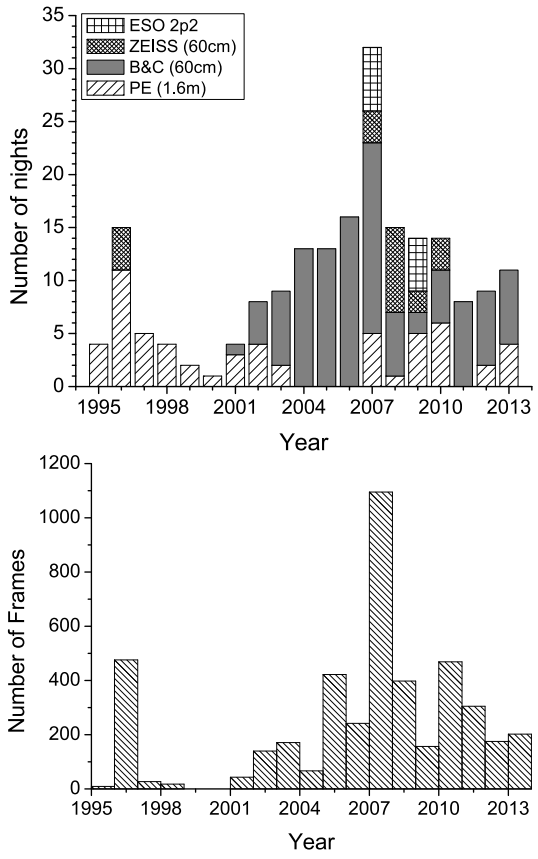

Fig. 2. *Top*: distribution of nights grouped by telescope. *Bottom*: number of frames taken per year.

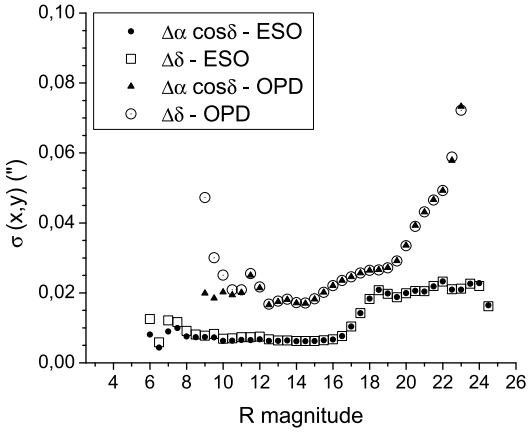

Fig. 3. (x, y) measurement errors as a function of R magnitude for all OPD and ESO telescopes sets. Values are averages in 0.5 mag bins.

Table 2. Astrometric (α, δ) reduction for each observational telescope set.

Telescope	Mean errors σ_α mas	σ_δ mas	No. of frames	UCAC4 stars
Zeiss (60 cm)	32	57	833	131
Boller & Chivens (60 cm)	76	67	2837	235
Perkin-Elmer (1.6 m)	68	84	742	46
ESO/MPG/WFI (2.2 m)	53	52	145	2357

Notes. Mean errors are the standard deviations in the (O−C) residuals from (α, δ) reductions with the UCAC4 catalog.

Celestial Reference System (ICRS), and the six constants polynomial to model the (x, y) measurements to the (X, Y) tangent plane coordinates. To help identify Pluto in the frames and derive the ephemerides for the instants of the observations for future comparisons, we used the kernels from SPICE/JPL[4]. The Pluto system was represented by the DE421 + plu021[5] JPL ephemerides. Magnitudes were obtained from PSF photometry and calibrated with respect to the UCAC4.

Figure 3 shows the distribution of (x, y) errors as a function of R magnitude for all used OPD and ESO telescopes. The observational strategies optimized the imaging of Pluto and the UCAC4 reference stars, as can be seen by the smaller errors in the 13−16 mag range. The ESO observations take advantage of the larger telescope aperture, better seeing, and sky transparency. One by one, outlier reference stars were eliminated in an iterative reduction procedure, until all (O−C) position residuals were below 120 mas (about 3 times the UCAC4 error). No weights were used for the reference stars. The position mean errors from the (O−C)s (α, δ) reductions are listed in Table 2; the average number of reference stars and number of CCD frames are also given for each telescope set of observations.

The reduced positions minus Pluto ephemeris offsets serve to correct for differential chromatic refraction, and later to correct for the effect of the Pluto/Charon mixed PSFs. The details of these corrections are given in the following sections.

We recall that the DE421 and plu021 were the most modern ephemerides available for Pluto when this work started. Therefore, they are used throughout this work and, in particular, to obtain both corrections mentioned above. We show, in the following sections, that these corrections are not significantly affected by a change in the ephemerides used.

3.2. Differential chromatic refraction correction

Pluto has been, for an Earth-based observer, backgrounded by the Galactic plane since 2002. Thus, the mean color of the stars on the field tend to be redder than the light of the Sun reflected back by Pluto. This difference in color, if not taken into account, may induce a shift in the observed positions of up to 0.1″ due to differential color refraction.

The classical theory of refraction (Stone 1996) presents two terms for the correction. The first is due to the position of the observed objects and is a function of the latitude of the site (ϕ), of the object's declination (δ), and of the hour angle (H): $V_{\alpha,\delta}(\phi, \delta, H)$. The second term is due to the atmospheric conditions and the wavelength (λ) of Pluto and of the stars in the field: $B(\lambda)$.

The equations that represent the first part $V_{\alpha,\delta}(\phi, \delta, H)$ are given in Eqs. (1) and (2). Their behavior is shown in Fig. 4:

$$V_\alpha(\phi, \delta, H) = \frac{\sec^2\delta \cdot \sin H}{\tan\delta \cdot \tan\phi + \cos H}, \quad (1)$$

$$V_\delta(\phi, \delta, H) = \frac{\tan\phi - \tan\delta \cdot \cos H}{\tan\delta \cdot \tan\phi + \cos H}. \quad (2)$$

[4] Website: http://naif.jpl.nasa.gov/naif/toolkit.html

[5] See http://naif.jpl.nasa.gov/pub/naif/generic_kernels/spk/satellites/ for details on plu021 and its successors. In this work, ephemerides named pluXXX are used solely to describe the orbits of Pluto and Charon around the barycenter of the Pluto system.

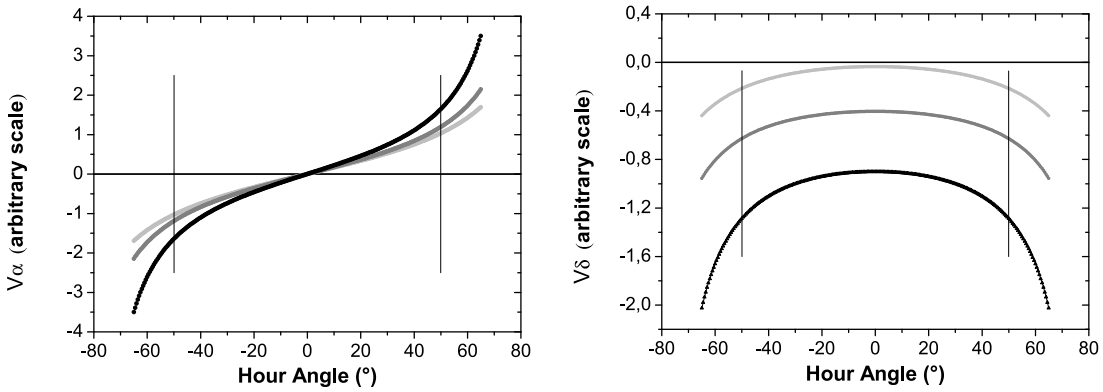

Fig. 4. Behavior of the $V_\alpha(\phi, \delta, H)$ (*left*) and $V_\delta(\phi, \delta, H)$ (*right*) functions for a latitude of $\phi = -22°$ and using the same arbitrary scale. We noted that the chromatic refraction is more effective in right ascension than in declination. The vertical lines indicate the limits in hour angle of our observations. The light gray curve represents a declination of $-20°$; the gray curve represents a declination of $0°$; and the black curve represents a declination of $+20°$.

A typical field of view (FOV) of a few arc-minute sizes is small enough so that the differential variations of $V_\alpha(\phi, \delta, H)$ and $V_\delta(\phi, \delta, H)$ along the FOV can easily be taken into account by applying the usual polynomial models without color terms (like the six constant model we used), for relating the (x, y) and (X, Y) coordinates in the (α, δ) reductions.

On the other hand, taking into account the contribution of the other term $B(\lambda)$ directly in the model of the (α, δ) reductions is usually undesirable or impractical because of the increase of variables in the model in contrast to the limited number of reference stars, and because of the frequent lack of knowledge of the color of the reference stars and target.

However, since atmospheric conditions usually do not have large variations during one night, the term $B(\lambda)$ will basically depend upon the color of Pluto and of the average color of the stars, each of which is constant for one night and for a specific telescope/filter configuration. Thus, the remaining differential refraction effects in the positions of Pluto, not eliminated in the first step of the (α, δ) reductions, can now be removed past the reduction.

Assuming that the average $V_\alpha(\phi, \delta, H)$ and $V_\delta(\phi, \delta, H)$ terms from each star equals the respective ones for Pluto – which is true for the typical small FOV sizes of this work – we can model the position offsets as a function of the differential chromatic refraction $\triangle B$ between the stars and Pluto, as shown in Eq. (3):

$$\Delta[\alpha, \delta] = V_{\alpha,\delta}(\phi, \delta, H) \cdot \triangle B. \quad (3)$$

A standard least squares procedure was then used to determine the values of the $\triangle B$ term for each night and each color filter used on the observations (V, R, I, and Clear).

Figure 4 shows that the position variation in right ascension is much larger than that for declination as a consequence of Pluto's declination and the latitude of the OPD, and so, in practice, we first fitted $\triangle B$ using the equations in right ascension. Then we applied the fitted $\triangle B$ to eliminate the differential chromatic refraction from the declinations of Pluto. We note that the position variation in right ascension must be null at the meridian. Thus, we added a constant to the fit in right ascension, allowing for the presence of a true ephemeris right ascension offset. The fitted parameters from the model were used to remove the differential chromatic refraction from the right ascensions and declinations of Pluto.

After the computation of the terms $\triangle B$, for nights with more than 1^h30^{min} of observation (continuous or time spaced) we saw that the values obtained were coherent with those obtained for the same filter, presenting a small standard deviation about a mean value. Then, we separated our observations into two groups: nights in which $\triangle H > 1^h30^{min}$, and nights in which $\triangle H < 1^h30^{min}$. For the first group, we made corrections using the value of $\triangle B$ obtained for each night. The second group was corrected by using the average value of $\triangle B$ obtained for the respective filter. The values obtained for $\triangle B$ for each filter used are presented in Table 3. An example of the correction for one night is shown in Fig. 5.

Table 3. $\triangle B$ term in the differential chromatic refraction correction for each filter.

Color filter	$\triangle B$
Clear	0.086 ± 0.023
V	0.095 ± 0.015
R	0.053 ± 0.004
I	0.049 ± 0.012

In Fig. 5, the relevant parameter for the differential chromatic correction is the angular coefficient as determined from the gray dots. Since they are spread along an interval of a few hours only, the use of different ephemerides implies a constant displacement of these dots along the y-axis so that the angular coefficient remains unchanged. In fact, the differences between DE421 and DE430, INPOP13c, ODIN1 (where these ephemerides were used in combination with plu043[6]) is almost constant, with a dispersion of 2 mas. As shown in Sect. 5, the use of plu043 is done without loss of generality.

3.3. Photocenter correction

Pluto's main satellite, Charon, is approximately half its size. Their apparent angular separation in the sky is smaller than $1''$. Without enough angular resolution, the image that we obtain in the CCD frame is a mix of Pluto and Charon PSFs. The resulting PSF can be described by two overlapped Gaussians, with different maxima and non-coincident centers, one corresponding to Pluto and the other to Charon. Placing the Pluto Gaussian at the origin, and considering the Charon Gaussian, separated by a distance d from Pluto, the resulting mixed PSF will present a photocenter offset from the origin by $x_{\rm phot}$. This photocenter offset depends on the peak of each Gaussian (related to the brightness

[6] The most modern JPL ephemeris for the system of Pluto at the time of this writing.

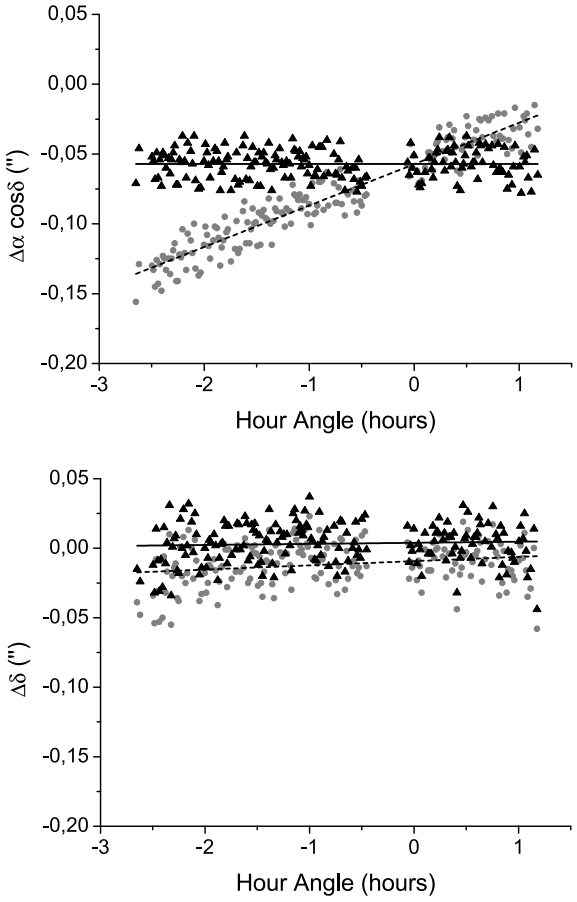

Fig. 5. An example of the differential chromatic refraction correction applied for one night of observations with the 0.6 m Bollen & Chivens OPD telescope on April 18, 2007 – in right ascension (*top*) and declination (*bottom*). Gray dots represent the position offsets with regard to the ephemeris before the correction and black triangles after. The dashed line is the linear fit to the data without the refraction correction, and the full line is the linear fit to the corrected data. On this plot, $\triangle B = 0.083$.

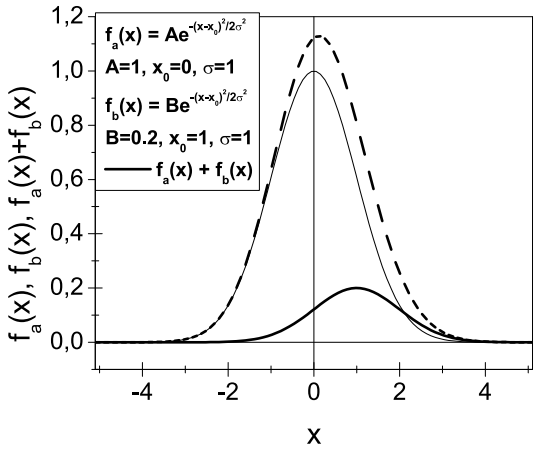

Fig. 6. Illustration of the Pluto/Charon photocenter problem: two Gaussian PSFs, $f_a(x) = A{\cdot}\exp[-(x-x_{a0})^2/2\sigma^2]$ and $f_b(x) = B{\cdot}\exp[-(x-x_{b0})^2/2\sigma^2]$ (full lines), are separated by a distance d. They overlap each other and result in the dashed line $f_a(x) + f_b(x)$, which is the observed mixed PSF. This PSF depends on the brightness ratio k and has a peak at a distance $x_{\rm phot}$ from the Pluto Gaussian which is centered at the origin. This term $x_{\rm phot}$ is the correction that we need to find to recover the Pluto photocenter from the measured photocenter of the mixed PSF. Here, as an illustration, $A = 1$, $B = 0.2$, $\sigma = 1$, $x_{a0} = 0$, and $x_{b0} = d = 1$.

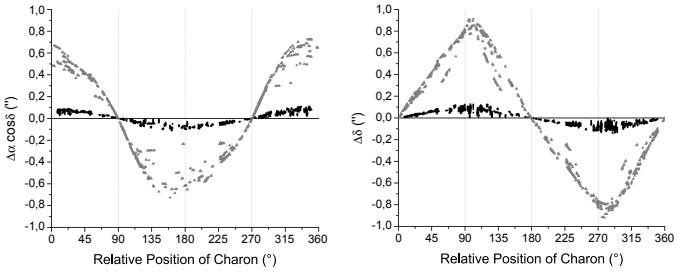

Fig. 7. In gray, Charon ephemerides positions (DE421+plu021) relative to Pluto for right ascension (*left*) and declination (*right*). In black, the corresponding photocenter correction presents the expected periodic behavior, but not in the same scale or function form. The dispersions in the plots for a given relative distance are due to the rotation of the apparent orbit of Charon projected in the sky, during the 19 years of our observations.

ratio k of the two bodies), on the FWHM (seeing) of the sky (related to the Gaussian σ by FWHM = 2.3588 σ), and on d itself. Then, the goal is to determine $x_{\rm phot}$ and, in a sense, to recover the true photocenter of Pluto from the measurement of the observed mixed PSF. An illustration of the problem is shown in Fig. 6.

After some developments, we derived expressions for the distance $x_{\rm phot}$ between the centers of the observed mixed PSF and the Pluto Gaussian. This photocenter correction is presented in Eq. (4). For a complete description of the developments of this equation, see Appendix A.

The actual photocenter corrections for right ascension and declination are the projections of Eq. (4) in the ($\triangle\alpha \cdot \cos\delta$, $\triangle\delta$) sky plane. These projections are given in Eqs. (6) and (7), respectively:

$$\frac{x_{\rm phot}}{d} = \gamma - \frac{\gamma - k\cdot(1-\gamma)\cdot\exp\left(d_\sigma^2\left(\gamma-\frac{1}{2}\right)\right)}{1 + k\left(d_\sigma^2(\gamma-1)+1\right)\cdot\exp\left(d_\sigma^2\left(\gamma-\frac{1}{2}\right)\right)}, \tag{4}$$

where

$$\begin{cases} \gamma = \frac{k}{\exp(\frac{d_\sigma^2}{2}) - k\cdot(d_\sigma^2-1)}, \\ d_\sigma = \frac{d}{\sigma}, \end{cases} \tag{5}$$

$$\Delta\alpha_{\rm phot}\cdot\cos\delta = x_{\rm phot}\cdot\cos\left(\tan^{-1}\left(\frac{Y_{\rm Charon}}{X_{\rm Charon}}\right)\right), \tag{6}$$

$$\Delta\delta_{\rm phot} = x_{\rm phot}\cdot\sin\left(\tan^{-1}\left(\frac{Y_{\rm Charon}}{X_{\rm Charon}}\right)\right), \tag{7}$$

where ($X_{\rm Charon}$, $Y_{\rm Charon}$) are the relative distances between Charon and Pluto, known from the ephemerides.

Figure 7 shows Charon's positions around Pluto, and the corresponding photocenter corrections obtained from actual observations. We find the expected periodic behavior, but the actual scale and function form of the corrections cannot be empirically derived by simplistic considerations, or solely based on the Pluto/Charon ephemeris relative distances, as we sometimes find in the literature.

The photocenter corrections depend on the brightness ratio k, but no precise values of k could be found in the literature for the

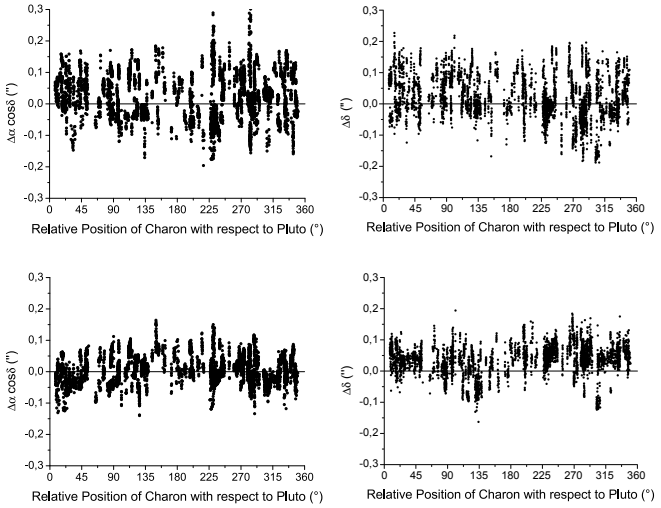

Fig. 8. Pluto ephemeris offsets before the photocenter correction (*top*) and after (*bottom*). Offsets for right ascension are on the *left*, declination offsets on the *right*.

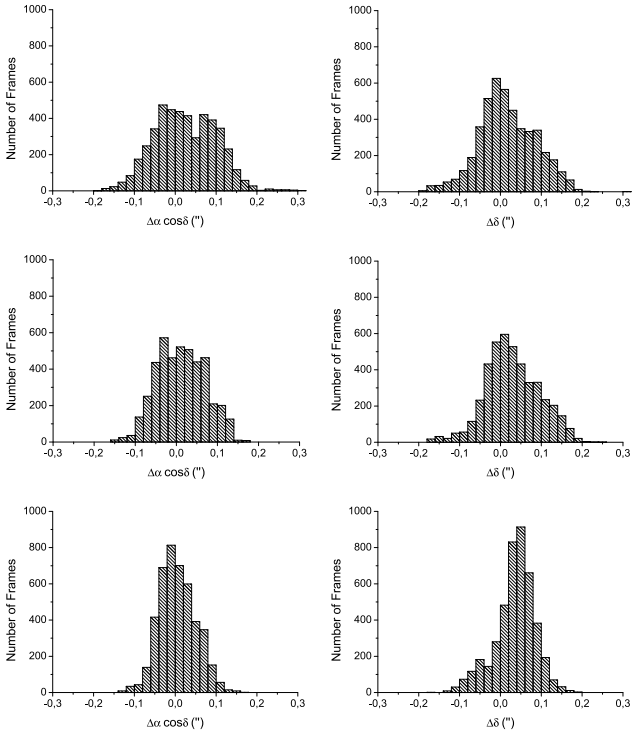

Fig. 9. Dispersion of Pluto's ephemeris offsets before (*top*) and after the differential chromatic refraction (*middle*) and Pluto photocenter corrections (*bottom*). Histograms of right ascension are on the *left* and of declination are on the *right*. Ephemeris positions refer to the DE421+plu021 ephemerides from JPL. We note, as explained in the two previous sections, that *the middle and bottom panels* do not need to be revisited under a change of ephemeris, given that our corrections are not dependent on ephemerides positions.

effective wavelengths of our telescope/filter sets. We partially solved this problem by simultaneously fitting k from the observations, in the process of determining the photocenter offsets $x_{\rm phot}$ (see details in Appendix A). After some tests, we found that the best fit for k comes from using all the data together. Separating the observations by filter (clear, I, R, ESO-R, V) gave the same results within 3σ, but with larger 1σ errors (about 0.04; 0.005 for clear). We also grouped the observations in many epoch bins and tested a number of possibilities, but the fits did not indicate conclusive variations in k, that could result from the slow rotation of the system and consequently gradual exposition of Pluto's pole during the 19 years of observations.

To refine the determination of k and $x_{\rm phot}$, we repeated the calculations after eliminating outlier points with large position minus ephemeris offsets, for which a 2σ filter was applied. Using all the remaining observations combined together, we obtained the final value for the brightness ratio: $k = 0.2106$ ($\sigma = 0.0014$). A 3σ filter was later applied to discard any surviving position outliers. The remaining 4557 points constituted the final set of Pluto positions of this work. Pluto ephemeris offsets before and after the photocenter corrections are shown in Fig. 8. we also noted that because Pluto's and Charon's albedos are not well known, and Pluto's albedo varies with observed phase, the value of k is an approximate value and does not remove completely the periodic behavior presented in Fig. 8. However, the value we obtained improves the correction for photocenter effect substantially, as can be seen in Figs. 7 and 8.

When making the comparison between different ephemerides for the system of Pluto (plu021, plu043, and ODIN1), the largest values come from the comparison between plu021 and ODIN1 in right ascencion, reaching 25 mas in absolute values, and values smaller than 5 mas from comparing plu043. For declination, all values are smaller than 8 mas. We also note, from Eq. (4), that the photocenter correction is dominated by the product of k (0.2106) and the distance Pluto-Charon. Therefore, the use of different modern ephemerides to describe the orbits of the system of Pluto would provide results differing by not more than about 5 mas from the ones presented here.

4. Results

The improvements in the final positions, measured by the dispersion of Pluto's ephemeris offsets after the two corrections described in Sects. 3.2 and 3.3, can be easily seen in the histograms in Fig. 9 and in the $\Delta\alpha \cdot \cos\delta$ vs. $\Delta\delta$ plot in Fig. 10. The same improvements in the positions can also be seen if different ephemerides are used.

After these corrections, we obtained a total of 4557 positions of Pluto. The complete table with positions and other data is available in electronic form at the CDS. A small sample is presented in Table 4. The table lists the Julian date of the observations (UTC), the final right ascension and declination corrected for differential chromatic refraction and photocenter offset, the total position errors, the observed apparent magnitude, the filter, the photocenter offsets in right ascension and declination, telescope used, and seeing. To retrieve the mixed positions of Pluto and Charon, corrected by differential chromatic refraction, one should subtract the furnished photocenter offsets from the listed final positions. Apparent magnitudes were computed from PSF fits with respect to the UCAC4, with errors of about 0.1 to 0.3 mag. The position errors listed in Table 4 were computed with Eq. (8):

$$P_{\rm error} = \sqrt{\sigma_1^2 + \sigma_2^2 + 0''.02^2}, \quad (8)$$

where σ_1 is the standard deviation of the ephemeris offset nightly averages and σ_2 is the error from the (x, y) measurements, computed from the Gaussian fits to the image profiles of

Table 4. Pluto's final positions corrected for chromatic refraction and for photocenter offset caused by Charon.

Date of observation	Pluto's final positions		Pos. errors		Mag.	Filter	Photocenter correction		Tel.	Seeing
	RA	Declination	σ_α	σ_δ			$\Delta\alpha\cos\delta$	$\Delta\delta$		
JD (UTC)	h m s	° ′ ″	″	″			″	″		″
2 449 937.41142361	15 54 32.5896	–06 31 10.005	0.027	0.039	14.196	*C*	–0.061	0.052	P	0.760
2 449 937.41465278	15 54 32.5899	–06 31 10.041	0.029	0.040	14.120	*C*	–0.033	0.137	P	0.979
⋮	⋮	⋮	⋮	⋮	⋮	⋮	⋮	⋮	⋮	⋮
2 456 509.67702687	18 39 30.6746	–19 57 58.238	0.025	0.030	14.809	*I*	–0.096	0.092	P	1.259
2 456 509.67740647	18 39 30.6733	–19 57 58.200	0.025	0.030	14.778	*I*	–0.095	0.074	P	1.059

Notes. The final right ascensions and declinations of Pluto are corrected for differential chromatic refraction and photocenter offset. To retrieve the positions of Pluto/Charon mixed in the images, corrected by differential chromatic refraction, subtract the furnished photocenter offsets from the listed final positions. The total position errors of the (α, δ)s are computed with Eq. (8) (see text). Apparent magnitudes were computed from PSF fits with respect to the UCAC4, with errors of about 0.1 to 0.3 mag. The designation of the filters are *V*, *R*, *I*, and *C* for clear (no filter). We note that *R* filters used at the OPD and the 2p2 telescopes are in different systems. The telescopes are identified as Z = Zeiss, B = Boller & Chivens, P = Perkin-Elmer, and M = ESO/WFI (see also telescope details in Sect. 2). Seeing refers to the average full width at half maximum (FWHM) of the seeing disk of the stars on each frame. Here, we sampled a few of the early and last observed positions. The complete data set is available at the CDS.

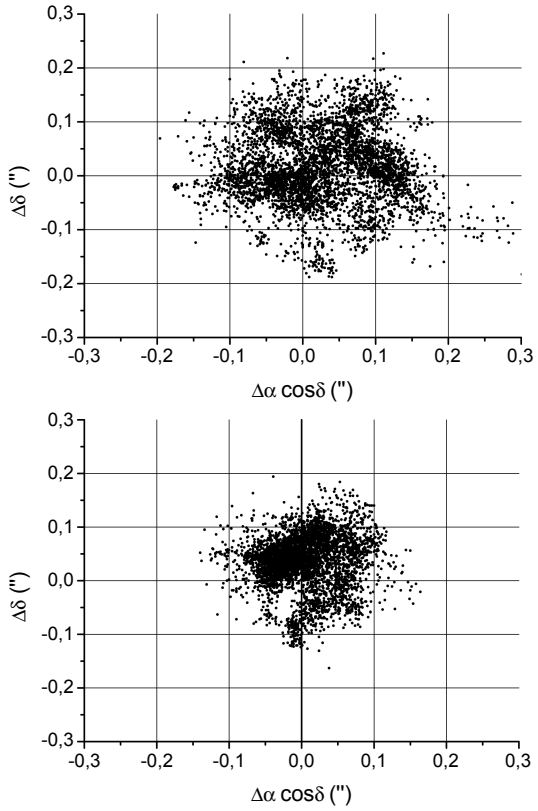

Fig. 10. Dispersion of Pluto's ephemeris offsets before (*top*) and after (*bottom*) the differential chromatic refraction and Pluto photocenter corrections. Ephemeris positions refer to the DE421+plu021 ephemerides from JPL.

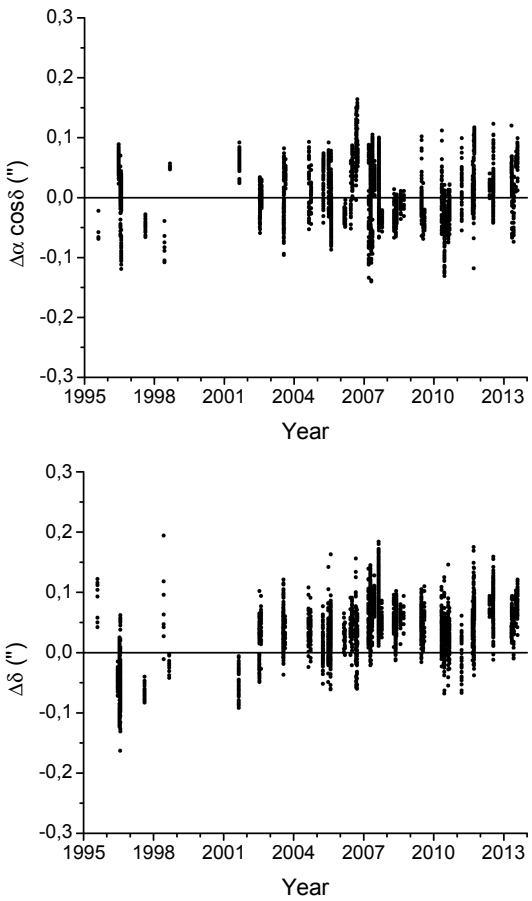

Fig. 11. Pluto's $\Delta\alpha\cos\delta$ (*top*) and $\Delta\delta$ (*bottom*) ephemeris offsets in the sense Pluto minus DE421+plu021, for the period from 1995 up to 2013. It is important to note the linear drift in declination from 2005 on, also obtained by Assafin et al. (2010) from stellar occultations.

Pluto/Charon. The value of 0.″02 accounts for systematic effects in UCAC4.

The applied corrections were able to improve the measured positions of Pluto, as shown by the sequence of panels in Fig. 9. The remaining systematic effects with respect to DE421+plu021 are believed to be offsets, as given, for instance, by the lower panel of Fig. 11 and confirmed by stellar occultations (see next section).

5. Comparison with ephemerides and stellar occultations

In the following sections, we compare our observations with stellar occultations and with DE421, DE430, INPOP13c, and ODIN1. We also show, for the pertinent period of time, that plu021, plu043, and ODIN1 describe the motions of Pluto

around the barycenter of its own system with good agreement. Therefore, improvements on the epmeherides of Pluto are achieved mainly with a better description of the motion of this barycenter around the solar system barycenter.

5.1. Comparison with DE421 and with stellar occultations results

The comparison of the final 4557 positions of Pluto with the DE421+plu021 gives ephemeris offsets (in the sense Pluto minus JPL) with mean values and standard deviations of +04 mas and σ_α = 45 mas and +37 mas and σ_δ = 49 mas for right ascension and declination, respectively. Figure 11 shows the obtained ephemeris offsets for the whole period (1995−2013). One can see an offset in declination that is no longer present in the more recent ephemerides considered here. We note that the results of stellar occultations (see Assafin et al. 2010) were used in INPOP13c and ODIN1, and that DE430 used both the positions presented here and the stellar occultation results.

It is interesting to note that this linear drift in declination from 2005 on is very similar to the drift presented by Assafin et al. (2010) based on stellar occultations. For a detailed analyzis of this result, we reduced a specific set of OPD images from past occultation campaigns, with observations of stars occulted by Pluto from 2005 to 2013. We obtained positions for 16 occulted stars by using the PRAIA package and the UCAC4 as reference catalog. The position results for these stars are shown in Table 5. They were determined by eliminating all the frames with exposure problems, usually presenting images with low signal-to-noise ratio, as well as those where there was an object close enough to contaminate the centroid determination of Pluto. Since the mean epoch of the position of the stars does not usually coincide with the date of the occultation, we applied UCAC4 proper motions, when available, to place the star position at the day of the occultation. The few remaining cases, where the UCAC4 proper motions were not available, USNOB-1 (second and fifth entries of Table 5; Monet et al. 2003), UCAC2 (third entry of Table 5; Zacharias et al. 2004), or the WFI catalogs for the Pluto system (twelfth entry of Table 5; Assafin et al. 2010) were used. Magnitudes in the R band were taken from the catalogs that provided the proper motions to the respective stars. This was done because many of these 16 stars had no observations with the R filter. The mean error refers to the standard deviations of the (O−C)s from the (α, δ) star reductions. The repeatability is the standard deviation about the average star position.

The relative distance of Pluto with respect to the star is determined with mas accuracy from the fitting of the light curves of stellar occultations. The distances for the events were determined by the group (Sicardy 2013, priv. comm.) which, adding our star positions to these distances, allowed us to obtain Pluto positions for these occultations. These Pluto positions are as precise as the positions derived for the stars themselves. Since we used the UCAC4, in principle we were able to derive better star positions i.e., Pluto ones, than the UCAC2-based positions of Assafin et al. (2010). We list these 16 Pluto positions in Table 5. We compared these Pluto positions with the JPL ephemerides DE421+plu021. The resulting ephemeris offsets are plotted in Fig. 12.

In Fig. 13, we plot the ephemeris offsets as a function of time for Pluto's positions directly derived from Pluto's ground-based observations (OPD and ESO). For comparison, we restricted the plot to 2005−2013. The 16 ephemeris offsets from occultations are also shown. We note the good agreement between the offsets shown in Figs. 12 and 13, particularly in declination.

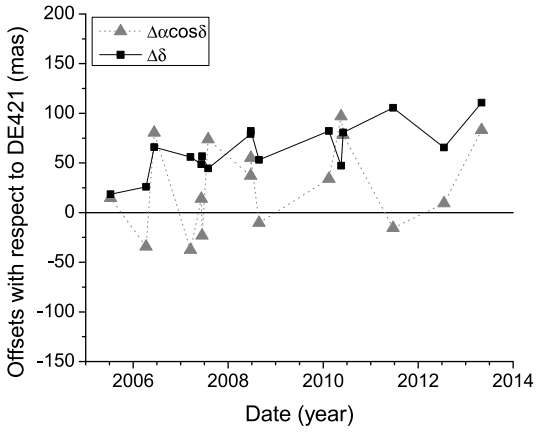

Fig. 12. JPL DE421+plu021 ephemerides offsets of Pluto in right ascension (triangles) and declination (squares) as a function of time, in the sense observed minus ephemeris. The 16 Pluto positions were determined from fittings of past occultations in 2005−2013, taking as reference the UCAC4-based star positions that we derived from OPD observations specifically made for these stars (see Table 5).

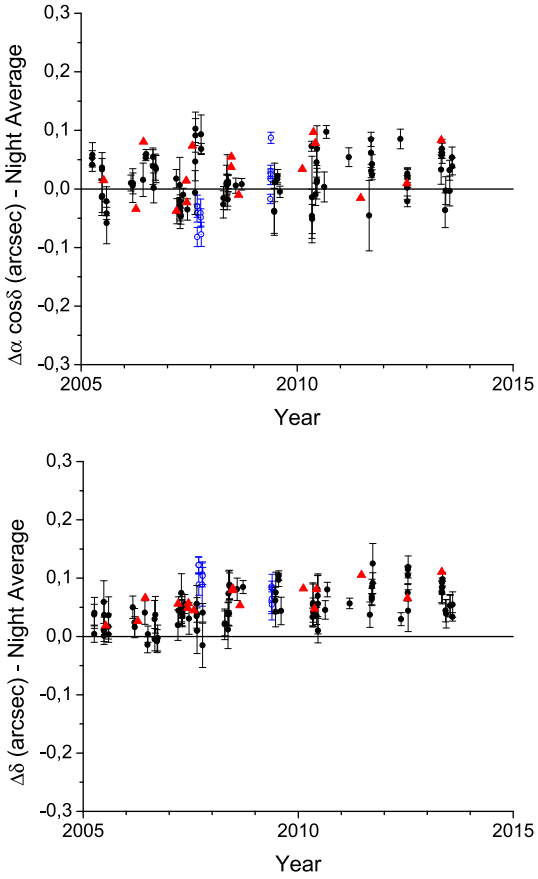

Fig. 13. Pluto's ephemeris offsets between 2005 and 2013, in the sense observed minus ephemeris (DE421+plu021), obtained from the OPD (black dots) and ESO (blue circles) observations. The 16 ephemeris offsets from the stellar occultations (red dots) are also shown. Right ascension is on *top* and declination is on the *bottom*. All offset sets are in agreement, particularly in declination.

Table 5. Precise Pluto positions based on 2005−2013 stellar occultations and on UCAC4-based star positions observed at OPD.

Occultation date	Star central observation epoch years	ICRS star positions RA h	Declination degrees	Mag R	Mean error σ_α mas	σ_δ mas	Repeatability E_α mas	E_δ mas	No. of frames	Pluto's offsets from stellar occultations $\Delta\alpha\cos\delta$ mas	$\Delta\delta$ mas	Geocentric positions of Pluto from occultations JD UTC	RA h	Declination degrees
2005 Jul. 11[a]	2013.532	17.481948800	−15.01518791	15.1	51	47	14	8	40	14.7	18.5	2 453 562.650983796	17.481944643	−15.01496958
2006 Apr. 10[b]	2006.162	17.768578025	−15.76946559	15.6	53	52	18	9	179	–34.2	25.9	2 453 835.713437500	17.768573370	−15.76963836
2006 Jun. 12	2013.532	17.686688372	−15.69289891	15.0	53	55	43	26	70	80.4	65.9	2 453 899.184375000	17.686688380	−15.69293003
2007 Mar. 18	2007.281	17.918248760	−16.47620446	15.2	54	53	15	14	663	–37.5	55.9	2 454 177.957812500	17.918247276	−16.47612781
2007 Jun. 09	2009.540	17.847403865	−16.37480759	16.4	55	56	37	18	73	14.0	48.7	2 454 260.900428241	17.847403854	−16.37482619
2007 Jun. 14	2006.646	17.839094971	−16.37838923	15.7	54	53	16	13	452	–23.2	56.8	2 454 265.560034722	17.839095024	−16.37838867
2007 Jul. 31	2006.715	17.761664371	−16.49212569	15.2	57	52	10	16	184	73.7	44.5	2 454 313.075752315	17.761665201	−16.49217792
2008 Jun. 22	2008.519	17.975837402	−17.04398606	12.5	57	49	17	23	93	37.1	79.2	2 454 640.299305555	17.975837607	−17.04403300
2008 Jun. 24	2008.519	17.972886881	−17.04703340	15.9	56	51	4	9	94	55.0	82.1	2 454 641.942928241	17.972886732	−17.04698831
2008 Aug. 25	2008.519	17.890861945	−17.25764839	16.0	53	54	11	8	68	–10.3	53.1	2 454 703.691099537	17.890860411	−17.25761219
2010 Feb. 14	2010.507	18.320660911	−18.27841969	10.6	58	58	21	8	71	34.0	82.1	2 455 241.700393518	18.320660719	−18.27836469
2010 May 19	2013.587	18.338000723	−18.19669245	17.1	57	58	78	9	164	96.9	47.2	2 455 335.745856482	18.338000944	−18.19672189
2010 Jun. 04	2010.479	18.313314917	−18.21438647	14.9	60	59	23	8	283	78.1	80.7	2 455 352.150752315	18.313314995	−18.21442508
2011 Jun. 23	2011.457	18.432076650	−18.80195362	14.5	58	56	2	2	76	–15.6	105.5	2 455 735.975115741	18.432076445	−18.80191986
2012 Jul. 18	2013.587	18.537408929	−19.40536793	14.6	59	58	8	13	214	9.3	65.5	2 456 126.676215278	18.537408960	−19.40537236
2013 May 04	2013.346	18.797926508	−19.69009352	14.3	57	54	10	15	86	83.1	110.7	2 456 416.849201389	18.797926607	−19.69010286

Notes. Precise star positions and geocentric Pluto positions for 16 stellar occultation dates between 2005−2013 are listed. The ICRS positions of the stars are given at noon of the occultation date in Col. 1. The mean error refers to the standard deviations of the (O−C)s from the (α, δ) star reductions. The repeatability is the standard deviation of the star position. All star positions were obtained using the UCAC4 as reference star catalog. The number of UCAC4 stars in each frame varies typically between 100 (for Perkin-Elmer) and 500 (for Zeiss and Boller & Chivens), depending on the size of the FOV. The epoch of the observation of the stars are given. The positions were corrected by UCAC4 proper motions, when available, to place the star positions at the occultation epochs given in the table. Proper motions from other catalogs were used otherwise (see text). Magnitudes in the R band were taken from the catalogs that provided the proper motions to the respective stars. The offsets on Pluto's positions, as obtained from the stellar occultations, are given with respect to DE421 and are in the sense observation minus DE421 (see Fig. 12). The positions of Pluto in the two last columns are geocentric astrometric positions in the ICRS, as obtained from stellar occultations (that is, corrected for the respective offsets). The associated JD is close (about 1s) to the geocentric closest approach. The relative geocentric distance of Pluto with respect to the star is determined with mas accuracy from the fitting of the light curves of stellar occultations. Adding our star positions to these distances allowed us to obtain the listed 16 Pluto positions for these occultations. These Pluto positions are as precise as the positions derived for the stars themselves. [(a)] This refers to an occultation by Charon. However, since the offset is mostly due to the planetary ephemeris DE421, rather than an offset in the orbit of Charon around Pluto as given by plu021, the same offset obtained for Charon can be applied to Pluto's position (see also Sicardy et al. 2006). [(b)] We note that there was no occultation on 2006 April 10 and this was actually predicted. The offsets could be derived due to high resolution adaptative optics observations of Pluto and the star made at the ESO-VLT 8 m Telescope UT4 (Paranal, Chile) – see Assafin et al. (2010).

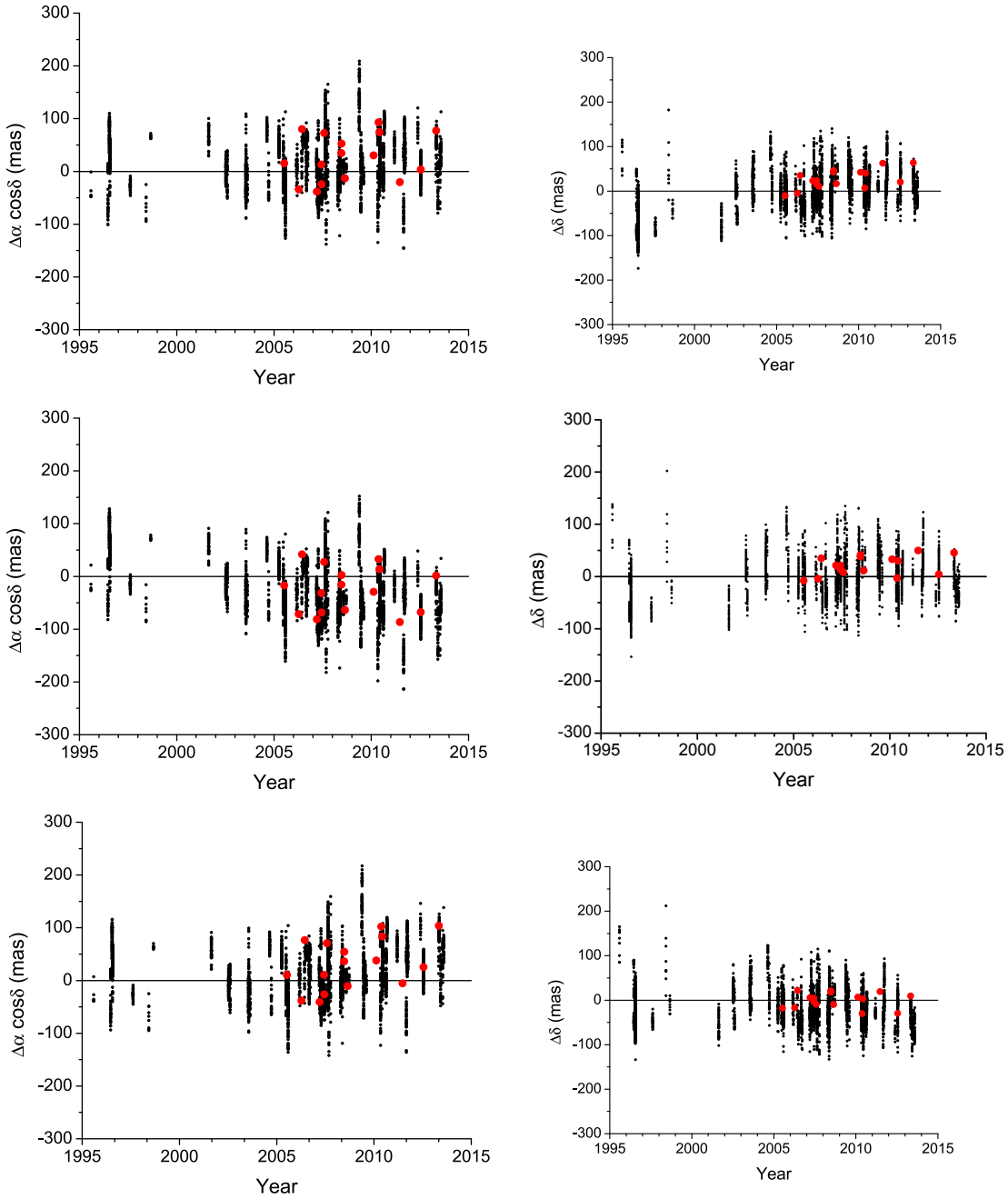

Fig. 14. *Upper panels*: differences in the sense observed minus DE430 positions of Pluto for right ascension (*left panel*) and declination (*right panel*). *Middle panels*: the same for INPOP13c. *Lower panels*: the same for ODIN1.

5.2. Comparison with more recent ephemerides

Figure 14 shows the differences in the sense observed minus ephemeris for recent ephemerides: DE430, INPOP13c, and ODIN1. We note that, compared to the lower panel in Fig. 11, the drift in declination is no longer present in the pertinent period of time. However, all these ephemerides used a set of positions for Pluto obtained from stellar occultations (Assafin et al. 2010) and/or the observations presented in this work. Therefore, it is expected that such an effect is no longer present.

In right ascension, the best agreement with the observations is given by the comparison with DE430. The mean values in right ascension over the pertinent period of time is 8 mas for DE430, −33 mas for INPOP13C, and 11 mas for ODIN1, with standard deviations of 48 mas, 54 mas, and 50 mas, respectively. In declination, the mean values are 0 mas, −2 mas, and −16 mas, and standard deviations are 43 mas, 39 mas, and 37 mas respectively. We note that the use of plu043 provides the most modern ephemerides for Pluto and does not prevent us from making a fair comparison between Figs. 14 and 11. Recent ephemerides describing the motion of Pluto around the barycenter of its own system are in good agreement, presenting a variation smaller than 4 mas for both right ascension and declination.

6. Conclusions

We obtained more than 4500 positions for Pluto spanning 19 years of observations at OPD/LNA and at ESO (Table 4). All the positions were obtained using the PRAIA package with the UCAC4 as the reference catalog. Two post reduction corrections

were applied: differential chromatic refraction and Pluto photocenter offset. The first was to correct the difference in color between Pluto and the reddened background reference stars (Pluto is crossing the Galactic plane). The second was to account for an offset in Pluto's measured photocenter, caused by the presence of Charon (Pluto/Charon separation in the sky plane is less than 1″). The second correction was done using a new, rigorous method based on the analyzis of PSFs (see a detailed description in Appendix A). Application of these corrections improved the precision of Pluto positions by a factor of two.

We also derived 16 precise positions for Pluto based on past stellar occultation results and on specific OPD observations for the occulted stars. These results agree with the 4557 derived Pluto positions from the OPD and ESO observations. In particular, we confirm the linear drift in declination from 2005 on, first pointed out in Assafin et al. (2010). It amounted to 100 mas in 2013.

We compared our positions of Pluto with the JPL planetary ephemeris DE421+plu021 and with more recent ephemerides. This comparison makes evident the improvement brought by the recent ephemerides and the importance of the positions presented here as well as the astrometry from stellar occultations.

This work is of significance for the navigation of the NASA New Horizons spacecraft. The positions obtained here were used to improve Pluto's orbit in the new JPL ephemeris DE430.

Acknowledgements. G.B.R. thanks CAPES/MEC for the partial support of this work. J.I.B.C., M.A., F.B.-R. and R.V.M acknowledge CNPq grants 302657/2010-0, 482080/2009-4, 478318/2007-3, 304124/2007-9 and 150541/2013-9. F.B.-R. acknowledges the support of the French-Brazilian Doctoral College Coordination of Improvement of Graduated Personnel program (CDFB/CAPES).

Appendix A: Development of the expressions of the photocenter correction

As presented in Sect. 3.2, Eq. (4) is the correction for the influence of Charon on the determination of Pluto's center. The problem arises when there is not enough angular separation to clearly differentiate Pluto and Charon in the image. Thus, one measures the combined photocenter of the two mixed PSFs. This problem can be described by the sum of two overlapping Gaussian functions (representing the PSF of isolated images), with different amplitudes and non-coincident centers, one corresponding to Pluto and the other to Charon. Placing the Pluto Gaussian at the origin, the influence of the Charon Gaussian, separated by a distance d, will depend on the amplitude of each Gaussian – related to the brightness ratio k of the two bodies – and on the σ of the two Gaussians (that is, on the FWHM, or seeing of the field stars, as $FWHM$ = seeing = 2.3588 σ). The goal, then, is to find the separation $x_{\rm phot}$ between Pluto's true center and the measured photocenter of the combined Pluto/Charon PSFs.

We start with the sum of two Gaussian functions with different amplitudes A and B:

$$f_{A+B}(x) = A \cdot \exp\left(\frac{-x^2}{2\sigma^2}\right) + B \cdot \exp\left(\frac{-(x-d)^2}{2\sigma^2}\right). \tag{A.1}$$

To find the maximum of the added PSFs, the derivative must be equal to zero:

$$\frac{\mathrm{d}\left(f_{A+B}(x)\right)}{\mathrm{d}x} = 0. \tag{A.2}$$

Thus,

$$\frac{A \cdot \exp\left(\frac{-x^2}{2\sigma^2}\right)}{\sigma^2}\left[-\frac{B(x-d)}{A} \cdot \exp\left(\frac{-d^2+2xd}{2\sigma^2}\right) - x\right] = 0\,, \tag{A.3}$$

Since the term outside the brackets is always greater than zero, the second part then must be zero:

$$\frac{B(x-d)}{A} \cdot \exp\left(\frac{-d^2+2xd}{2\sigma^2}\right) + x = 0\,. \tag{A.4}$$

To obtain the value of x that satisfies the previous equation, we use Newton's method to obtain the zeros of a function. We then set the initial value of the method to $x = 0$, to have a good approximation for the second iteration. Through this method, we find the equations for the two first iterations, given by Eqs. (A.3) and (A.4):

$$\triangle x_0(0) = \frac{kd}{\alpha - k\beta}\,, \tag{A.5}$$

$$\triangle x_1(\triangle x_0) = \frac{\alpha\triangle x_0 - k(d-\triangle x_0)\exp\left(d_\sigma^2\triangle x_{d0}\right)}{\alpha\sigma^2 - k(d_\sigma^2 - d_\sigma^2\triangle x_{d0} - \sigma^2)\exp\left(d_\sigma^2\triangle x_{d0}\right)}\,, \tag{A.6}$$

where

$$d_\sigma = \frac{d}{\sigma}, \quad \beta = d_\sigma - 1,$$
$$\alpha = \exp\left(\frac{d_\sigma^2}{2}\right), \quad \triangle x_{d0} = \frac{\triangle x_0}{d}. \tag{A.7}$$

The final solution for $x_{\rm phot}$ is then the sum of all the values for the iterations:

$$x_{\rm phot}(k,d,\sigma) = \sum x_i = x_0 + \triangle x_0 + \triangle x_1 + \ldots\,. \tag{A.8}$$

If we now substitute $x_0 = 0$, and use Eqs. (A.5) and (A.6), we have the expression for the photocenter correction:

$$x_{\rm phot}(k,d,\sigma) = \left(\frac{kd}{\alpha - k\beta}\right) + \left(\frac{\alpha\triangle x_0 - k(d-\triangle x_0)\exp\left(d_\sigma^2\triangle x_{d0}\right)}{\alpha\sigma^2 - k(d_\sigma^2 - d_\sigma^2\triangle x_{d0} - \sigma^2)\exp\left(d_\sigma^2\triangle x_{d0}\right)}\right). \tag{A.9}$$

To obtain the values of $x_{\rm phot}$, we now need three quantities: 1) the relative distance d between Pluto and Charon, given by the ephemerides; 2) the σ, related to the seeing of the stars in the field; and 3) the brightness ratio k, which is not well known. To get the best value of k from our observations, we consider $k = k_0 + \triangle k$, where k_0 is an initial value (best estimate) and $\triangle k$ the correction in first order to the value of k. Now, Eq. (A.9) can be rewritten as an approximation in first order:

$$x_{\rm phot}(k_0+\triangle k,d,\sigma) = \left[\triangle x_0(k_0) + \frac{\mathrm{d}\left[\triangle x_0(k_0)\right]}{\mathrm{d}k}\cdot\triangle k\right] + \left[\triangle x_1(k_0) + \frac{\mathrm{d}\left[\triangle x_1(k_0)\right]}{\mathrm{d}k}\cdot\triangle k\right]. \tag{A.10}$$

The variation of $\triangle x_1$ with respect to $\triangle x_0$ is very small, so deriving Eqs. (A.5) and (A.6) with respect to k and substituting in Eq. (A.10) gives

$$x_{\rm phot}(k_0+\triangle k,d,\sigma) = \left[\frac{k_0 d}{\alpha - k_0\beta} + \frac{\alpha d\triangle k}{(\alpha - k_0\beta)^2}\right] + \triangle x_1(k_0,d) - \frac{\alpha\cdot\left(\beta\triangle x_0 - d + \triangle x_0 - \frac{d_\sigma^2\triangle x_0^2}{d}\right)\cdot\exp\left(d_\sigma^2\triangle x_{d0}\right)}{\alpha - k_0\cdot(\beta - d_\sigma^2\triangle x_{d0})\cdot\exp\left(d_\sigma^2\triangle x_{d0}\right)}\cdot\triangle k. \tag{A.11}$$

Now, separating the zero and first order terms in $\triangle k$ furnishes a simple equation for $x_{\rm phot}$:

$$x_{\rm phot}(k_0 + \triangle k, d, \sigma) = \Phi^0 + \Phi^1 \triangle k \,. \tag{A.12}$$

To calculate the best value of k and the correction $x_{\rm phot}$, we use an initial value k_0 onto Eq. (A.11) and determine the value of $\triangle k$ iteratively until $\triangle k = 0$, so that the final correction will only depend on Φ^0, which is given by Eq. (A.13):

$$x_{\rm phot}(k_0, d, \sigma) = \Phi_0(k_0, d, \sigma) = \frac{k_0 d}{\alpha - k_0\beta} - d \cdot \frac{\frac{k_0}{\alpha-k_0\beta} - \left(\frac{k_0}{\alpha} - \frac{k_0^2}{\alpha(\alpha-k_0\beta)}\right) \cdot \exp\left(\frac{k_0 d_\sigma^2}{\alpha-k_0\beta}\right)}{1 - \frac{k_0}{\alpha} \cdot \left(d_\sigma^2 - \frac{k_0 d_\sigma^2}{\alpha-k_0\beta} - 1\right) \cdot \exp\left(\frac{k_0 d_\sigma^2}{\alpha-k_0\beta}\right)}. \tag{A.13}$$

The offsets in right ascension and declination can now be determined by the projections of $x_{\rm phot}$ considering Charon's positions around Pluto, or as in Eqs. (6) and (7):

$$\triangle\alpha \cdot \cos\delta_{\rm phot} = x_{\rm phot}(k_0, d, \sigma) \cdot \cos\left(\tan^{-1}\frac{Y_{\rm Charon}}{X_{\rm Charon}}\right), \tag{A.14}$$

$$\triangle\delta_{\rm phot} = x_{\rm phot}(k_0, d, \sigma) \cdot \sin\left(\tan^{-1}\frac{Y_{\rm Charon}}{X_{\rm Charon}}\right). \tag{A.15}$$

The elimination of outlier points – positions displaying large ephemeris offsets with regard to the nightly average – improves the determination of k and $x_{\rm phot}$. We repeated the procedure above with a 2-sigma clip procedure in order to clean the sample from outliers (see Sect. 3.2).

References

Assafin, M., Camargo, J. I. B., Vieira Martins, R., et al. 2010, A&A, 515, A32
Assafin, M., Vieira Martins, R., Camargo, J. I. B., et al. 2011, in Gaia follow-up network for the solar system objects: Gaia FUN-SSO workshop proceedings, held at IMCCE, Paris Observatory, France, November 29–December 1, 2010, eds. P. Tanga, & W. Thuillot, 85
Assafin, M., Camargo, J. I. B., Vieira Martins, R., et al. 2012, A&A, 541, A142
Beauvalet, L., Robert, V., Lainey, V., Arlot, J.-E., & Colas, F. 2013, A&A, 553, A14
Bessell, M. S. 1990, ASP, 102, 1181
Buie, M. W., Tholen, D. J., & Horne, K. 1992, Icarus, 97, 211
Camargo, J. I. B., Vieira-Martins, R., Assafin, M., et al. 2014, A&A, 561, A37
Christy, J. W., & Harrington, R. S. 1978, AJ, 83, 1005
Eichhorn, H., & Williams, C. A. 1963, AJ, 68, 221
Elliot, J. L., Dunham, E. W., Bosh, A. S., et al. 1989, Icarus, 77, 148
Fienga, A., Manche, H., Laskar, J., & Gastineau, M. 2008, A&A, 477, 315
Fienga, A., Laskar, J., Verma, A., Manche, H., & Gastineau, M. 2012, in SF2A-2012: Proc. of the Annual meeting of the French Society of Astronomy and Astrophysics, eds. S. Boissier, P. de Laverny, N. Nardetto, et al., 25
Fienga, A., Manche, H., Laskar, J., Gastineau, M., & Verma, A. 2013 [arXiv:1301.1510]
Fienga, A., Manche, H., Laskar, J., Gastineau, M., & Verma, A. 2014 [arXiv:1405.0484]
Folkner, W. M., Williams, J. G., & Boggs, D. H. 2009, Interplanetary Network Progress Report, 178, 1
Folkner, W. M., Williams, J. G., Boggs, D. H., Park, R. S., & Kuchynka, P. 2014, Interplanetary Network Progress Report, 196, C1
Harrington, R. S., & Christy, J. W. 1980, AJ, 85, 168
Leonard, F. C. 1930, ASP Leaflet, 1, 121
Monet, D. G., Levine, S. E., Canzian, B., et al. 2003, AJ, 125, 984
Nicholson, S. B., & Mayall, N. U. 1931, AJ, 73, 1
Rapaport, M., Teixeira, R., Le Campion, J. F., et al. 2002, A&A, 383, 1054
Roush, T. L., Cruikshank, D. P., Pollack, J. B., Young, E. F., & Bartholomew, M. J. 1996, Icarus, 119, 214
Showalter, M. R., Hamilton, D. P., Stern, S. A., et al. 2011, IAU Circ., 9221, 1
Showalter, M. R., Weaver, H. A., Stern, S. A., et al. 2012, IAU Circ., 9253, 1
Sicardy, B., Bellucci, A., Gendron, E., et al. 2006, Nature, 439, 52
Sicardy, B., Braga-Ribas, F., Widemann, T., et al. 2012, in AAS/Division for Planetary Sciences Meeting Abstracts, 44, 30401
Slipher, V. M. 1930, J. Roy. Astron. Soc. Canada, 24, 282
Stern, S. A. 1992, Ann. Rev. Astron. Astrophys., 30, 185
Stone, R. C. 1996, ASP, 108, 1051
Stone, R. C. 2001, AJ, 122, 2723
Tombaugh, C. W. 1946, ASP Leaflet, 5, 73
Walker, A. R. 1980, MNRAS, 192, 47P
Weaver, H. A., Stern, S. A., Mutchler, M. J., et al. 2006, Nature, 439, 943
Young, L. A., & Stern, S. A. 2000, in Lunar and Planetary Inst. Technical Report, 31, 2081
Zacharias, N., Urban, S. E., Zacharias, M. I., et al. 2004, AJ, 127, 3043
Zacharias, N., Finch, C. T., Girard, T. M., et al. 2013, AJ, 145, 44